Graz University of Technology

MeasureMINT: UWB Channel Measurement Campaigns

Performed by the Wireless Communications Group of the Signal Processing and Speech Communications Laboratory at Graz, University of Technology from 2010 to 2013. This document contains an overview of:

- Measurement Setup
- Measurement Scenarios

Authors: Paul Meissner, Erik Leitinger, Stefan Grebien, Josef Kulmer, Manuel Lafer, Klaus Witrisal

Date: Graz, December 19, 2023
Rev.: 2.0

Contents

1 Descriptions of Channel Measurement Campaigns

This section describes the various channel measurement campaigns that have been performed during the work on this thesis. These measurements are also publicly available for research purposes [MLLW13b]. In the following, Section 1.2 describes the different measurement setups, i.e. frequency- and time-domain measurements. Section 1.3 then discusses the possible options for signal postprocessing, while Sections 1.4, 1.5, and 1.6 contain the detailed descriptions of the various scenarios.

1.1 Overview

The main aim of the measurements campaigns described here is to evaluate the performance of indoor localization and tracking algorithms in realistic scenarios and to gather knowledge of the relevant propagation phenomena. Therefore, measurements are performed along trajectories, that model motion paths of moving agents. Such measurements are done in different representative environments. At each trajectory point, channel measurements with a certain number of fixed anchors are performed.
Table 1.1 contains an overview over all measurement campaigns. The different campaigns are divided into frequency- and time-domain measurements. The distinction is based on the measurement device that has been used. For all scenarios, the number of points on the measurement trajectories and their spacing are given. Also, the number of anchors used is indicated, which corresponds to the number of channels measured per trajectory point. For the frequency-domain measurements obtained with a vector network analyzer, the frequency resolution Δf is given. This is related to the maximum delay that can be represented unambiguously with these measurements, i.e. $\tau_{\max} = 1/\Delta f$. For the case of the time-domain measurements, the number of averages resulting in the measured signal at one trajectory position is given.
Table 1.2 shows an overview over published papers using the various measurements.

Frequency domain measurement campaigns – Vector Network Analyzer				
Scenario	**# Points**	**Spacing** [cm]	**Freq. res.** Δf [MHz]	**#Anchors**
Corridor (Fig. 1.2)	381	10	1	6
Corridor, Grid (Fig. 1.2)	484	5	1.5	2
Seminarroom, bistatic (Fig. 1.4)	2x220	5	5	2
Seminarroom, monostatic (Fig. 1.4)	2x220	5	5	0
Lab, equipped (Fig. 1.9)	61	5	5	2
Lab, empty	61	5	5	2
Time domain measurement campaigns – M-sequence channel sounder				
Scenario	**# Points**	**Spacing** [cm]	**# Avg.**	**#Anchors**
Seminarroom, local grids (Fig. 1.4)	2x220x25	1	1024	2
Demo room Graz (Fig. 1.7)	101, 235	5	33	4
Demo room Montbeliard (Fig. 1.8)	154, 161	3	33	2

Table 1.1: Available Measurement Campaigns and Parameters

Scenario	**Publication**	**Comments**
Corridor (Fig. 1.2)	[MLFW13]	Tracking using measurements Comparison with conventional algorithms
	[MW12a]	Experimental computation of bounds Estimation of MPC SINRs based on measurements
	[MW12b]	Tracking using measurements
	[MAGW11a]	Energy capture analysis of det. MPCs
	[MAGW11b]	Same, extended results
	[FMGW11]	MPC estimation, extension of [SKA$^+$10] to VA model
	[FMW12]	MPC tracking using PHD filters
Corridor, Grid (Fig. 1.2)	[MGM$^+$13]	Validation of ray-tracing
Seminarroom (Fig. 1.4)	[MLW14]	Tracking and channel estimation
	[LFMW14]	Tracking and channel estimation
Laboratory room (Fig. 1.9)	not yet used	
Demo room Graz (Fig. 1.7)	[MLLW14]	Description of demonstration system
Room Montbeliard(Fig. 1.8)	[MLLW13a]	Live demonstration
	[MLLW14]	Description of demonstration system

Table 1.2: Overview over publications using the measurement campaigns

1.2 General Measurement Setup

For both frequency- and time-domain measurements, Skycross SMT-3TO10M UWB antennas as well as custom made antennas using Euro-cent coins [Kra08] have been used. Those antennas have an approximately uniform radiation pattern in azimuth domain and zeroes in $\pm 90\,^\circ$ elevation. They are mounted on tripods in a height of $1.5 - 1.8\,\mathrm{m}$, depending on the scenario. The cables were Huber & Suhner Sucoflex or S-Series cables, which each have an attenuation of approximately 1.1 dB per meter at a frequency of 10 GHz and 1.6 dB per meter at 18 GHz.
A static environment has been ensured in all scenarios, i.e. there have been no moving persons or

objects. All floor plans that are shown have been measured by hand using a laser distance meter and a tape measure. The two-dimensional representation corresponds to the room dimensions in the height at which the antennas have been mounted.

1.2.1 Frequency Domain Measurements – Vector Network Analyzer

Frequency-domain measurements have been obtained with a *Rhode & Schwarz ZVA-24* VNA. The frequency range has been chosen as the full FCC bandwidth from 3.1 to 10.6 GHz (corresponding to a wavelength range of 9.67 cm to 2.83 cm), resulting in a delay resolution of 0.1333 ns and a spatial resolution of 4 cm. At the ℓ-th trajectory position, a sampled version $H_\ell[k]$ of the CTF $H_\ell(f)$ with a frequency spacing of Δf is measured.
The VNA has been calibrated up to (but not including) the antennas with a through-open-short-match (TOSM) calibration. The FCC bandwidth has been measured for different discrete frequencies, depending on the frequency resolution of the respective campaign (see Table 1.1). A resolution bandwidth of 10 kHz has been used for each campaign. The transmit power has been set to 15 dBm.

1.2.2 Time Domain Measurements – M-Sequence Radar

Time-domain measurements have been obtained with an *Ilmsens Ultra-Wide Band M-Sequence device* [SHK+07]. The measurement principle is correlative channel sounding [Mol05]. A binary code sequence with suitable autocorrelation properties (a large peak-to-off-peak-ratio) is transmitted over the channel. At the receiver, the channel impulse response is recovered using a correlation with the known code sequence.
This M-sequence radar has one transmitter and two receiver ports. Hence, the mobile unit that has been moved along the measuerement trajectories was the transmitter, and the two receiver ports have been used as anchors. The transmit power of the M-sequence device in FCC mode is 18 dBm. The employed 12-bit M-sequence has a length of 4095 samples. At the clock rate of 6.95 GHz, this allows for a maximum delay of $\tau_{\max} = 589.2$ ns.

1.3 Measurement Post-Processing

1.3.1 Frequency Domain Measurements – Vector Network Analyzer

For the VNA measurements, the major system influences on the measured CTF $H(f)$ have already been removed by the previously mentioned TOSM calibration. This includes cables and connectors, but not the antennas, which are considered as part of the transmission channel. The necessary post-processing tasks reduce to a filtering of the signal to select a desired frequency band out of the FCC range and to downconvert the signal transformed to time domain to obtain a baseband signal. The filtering is done with a baseband pulse $s(t)$ that covers the desired bandwidth.
The CTF is measured at N_f discrete frequencies $f_k = k\Delta f + f_{\min},\ k = 0, \ldots, N_f - 1$, where $f_{\min}$ is the lowest measured frequency. This sampled CTF $H[k]$ corresponds to a Fourier series representation of the time-domain CIR $h(\tau)$ [MLFW13], which is periodic with a period of $\tau_{\max}$. With f_0 and f_c denoting the lower band edge and the center frequency of the extracted band, respectively, and using an IFFT with size $N_{\text{FFT}} = \left\lceil (\Delta f \Delta\tau)^{-1} \right\rceil$, where $\Delta\tau$ is the desired delay resolution, the time domain equivalent baseband signal is obtained as

$$r(t) = \text{IFFT}_{N_{\text{FFT}}} \left\{ H[k] S[k] \right\} \mathrm{e}^{-j2\pi(f_c - f_0)t}. \tag{1.1}$$

Here, $S[k]$ is the discrete frequency domain representation of the pulse $s(t)$ in the desired frequency range. This procedure is similar to [SKA+10].

1.3.2 Time Domain Measurements – M-Sequence Radar

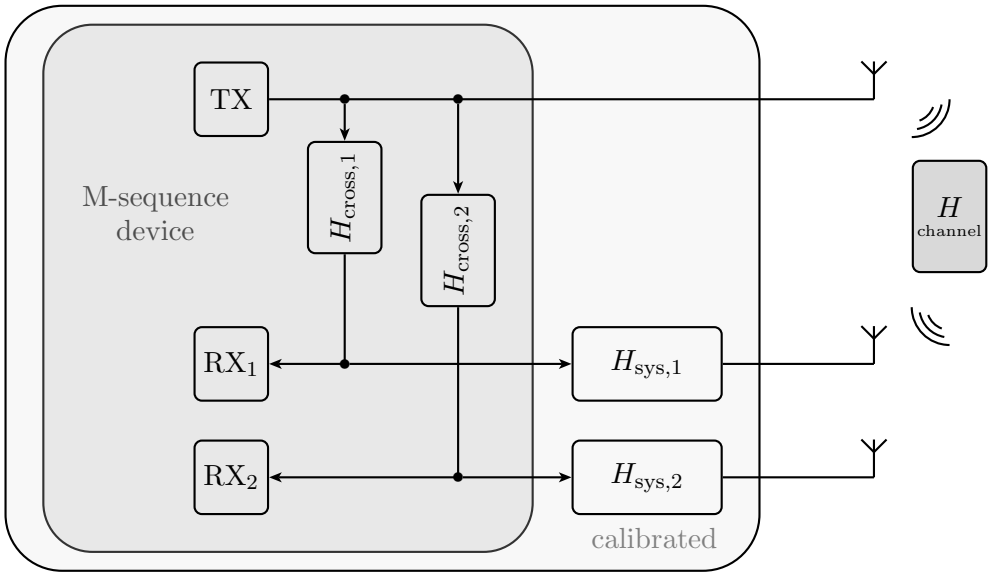

Figure 1.1: Calibration setup for time domain measurements

Fig. 1.1 shows a block diagramm of the measurement setup using the M-Sequence radar. As in the VNA measurements, the measurement system should be calibrated up to (but not including) the antennas. Hence, the influence of the device internal transfer functions and the measurement cables and connectors, combined in the transfer function $H_{\text{sys},i}(f)$ for the i-th RX channel, as well as the crosstalk between TX channel and i-th RX channel, $H_{\text{cross},i}(f)$, have to be compensated. For the further description, we will drop the channel index.
To achieve this, two types of measurements are necessary. First, to determine the crosstalk, the TX antenna is unmounted and the TX port is terminated with a $50\,\Omega$ match and the crosstalk signals are measured. Second, also the RX antennas are unmounted and TX and RX cables are connected. In this way, $H_{\text{meas}}(f) = H_{\text{sys}}(f) + H_{\text{cross}}(f)$ are measured. Using the measurement configuration with all the antennas as depicted in Fig. 1.1 yields $H_{\text{meas}}(f) = H(f)H_{\text{sys}}(f) + H_{\text{cross}}(f)$. Hence, a calibrated version of the radio channel transfer function is obtained as

$$H(f) = \frac{H_{\text{meas}}(f) - H_{\text{cross}}(f)}{H_{\text{sys}}(f) - H_{\text{cross}}(f)}. \tag{1.2}$$

To avoid excessive noise gain, we use a thresholding on the time-domain representation of the denominator in (1.2) and set samples below the threshold to zero. The time domain signal is obtained by an inverse Fourier transformation. Finally, the time-domain signal within the desired frequency range around the center frequency f_{c} can be computed using a suitable baseband pulse shape $s(t)$ as

$$r(t) = \left[h(t) * s(t)e^{j2\pi f_{\text{c}}t}\right] e^{-j2\pi f_{\text{c}}t} * \delta(t - \tau_{\text{shift}}). \tag{1.3}$$

Here, τ_{shift} is a time shift that accounts for the delays of connectors in the calibration measurements and the antennas, which have not been removed by (1.2). For connectors, this value

can be measured using a VNA, for the antennas, it can be computed using the length of the antennas and the propagation velocity in the materials, which is often given in data sheets. This calibration procedure is similar to [CPB07] and is also described in [Laf14].
The publicly available measurements [MLLW13b] contain extraction functions for Matlab, that directly deliver signals in the form of (1.3).

1.4 Large-Scale Environment – Corridor

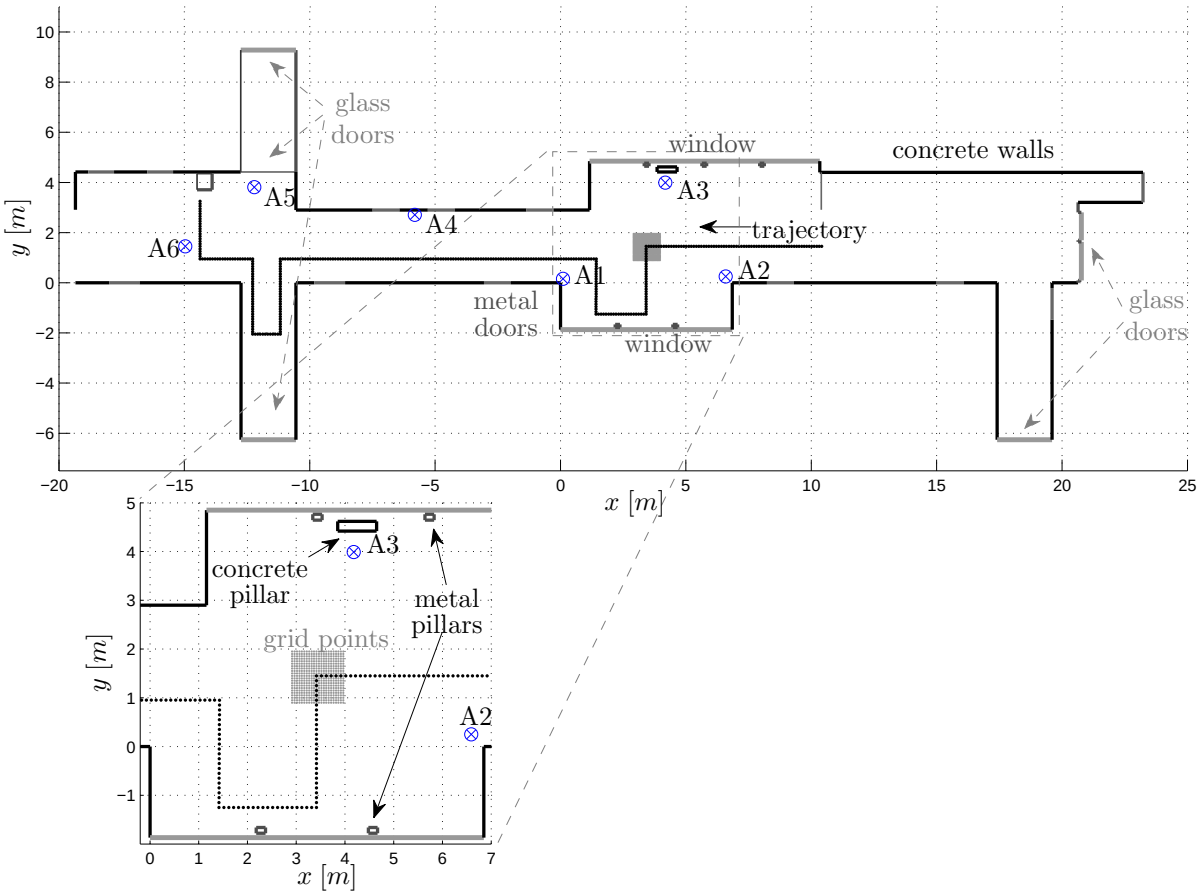

Figure 1.2: Large-scale measurement scenario in the corridor of the laboratory. In this scenario, six anchors are available, enabling the use of conventional localization algorithms. Two different measurement setups are used: 1) A trajectory with 381 points spaced by 10 cm, and 2) measurements within a grid of 484 points with 5 cm spacing. For the grid setup, only anchors 2 and 3 are available.

1.4.1 Trajectory Measurements

As shown in Figs. 1.2 and 1.3, these measurements have been obtained in a large corridor in our university building. The mobile was moved over a distance of almost 40 m (381 points, spaced by 10 cm) with measurements to six anchor nodes. Position 1 is at the right side. Mobile and Anchors 1 and 4 were equipped with the Skycross antennas, the other anchors with the coin antennas. All antennas were mounted at a height of 1.5 m.
Different LOS/NLOS conditions over this long distance allow for detailed performance evaluations of tracking algorithms. In this scenario, building walls are made of reinforced concrete and

the doors of metal. It is an open, three-storey building with some metal bridges connecting the two sides of the corridor, as seen in Fig. 1.3.

1.4.2 Grid Measurements

As shown in Figs. 1.2, also grid measurements have been obtained in this scenario to allow for local channel analysis. In an area of roughly 1 m^2, 484 (22x22) points with a spacing of 5 cm have been obtained to anchors 2 and 3. Position 1 is at the lower left side, position 22 at the lower right side and position 484 at the upper right side. For the grid measurements, all anchors and the mobile were equipped with the coin antennas and mounted at a height of 1.5 m.

Figure 1.3: Photo of corridor scenario, view approximately from the letter "y" in "trajectory" in Fig. 1.2.

1.5 Medium-Scale Environments

1.5.1 Seminarroom at Graz University of Technology

Figs. 1.4 and 1.5 illustrate a seminarroom at our university. As shown, different wall materials are present as well as a solid concrete pillar on the left side, which creates a short NLOS region w.r.t. Anchor 1 and Mobile 2. Two trajectories are measured, also the measurements between the two mobiles are available to evaluate cooperative algorithms. For all anchors and mobiles, the coin antennas were used, mounted at a height of 1.23 m.
In a second measurement run, also monostatic measurements of both mobiles have been obtained, i.e. measurements where TX and RX are at the same location. For this purpose, an antenna setup as shown in the right plot of Fig. 1.5 has been used to allow for a low direct coupling between the TX and RX antennas.

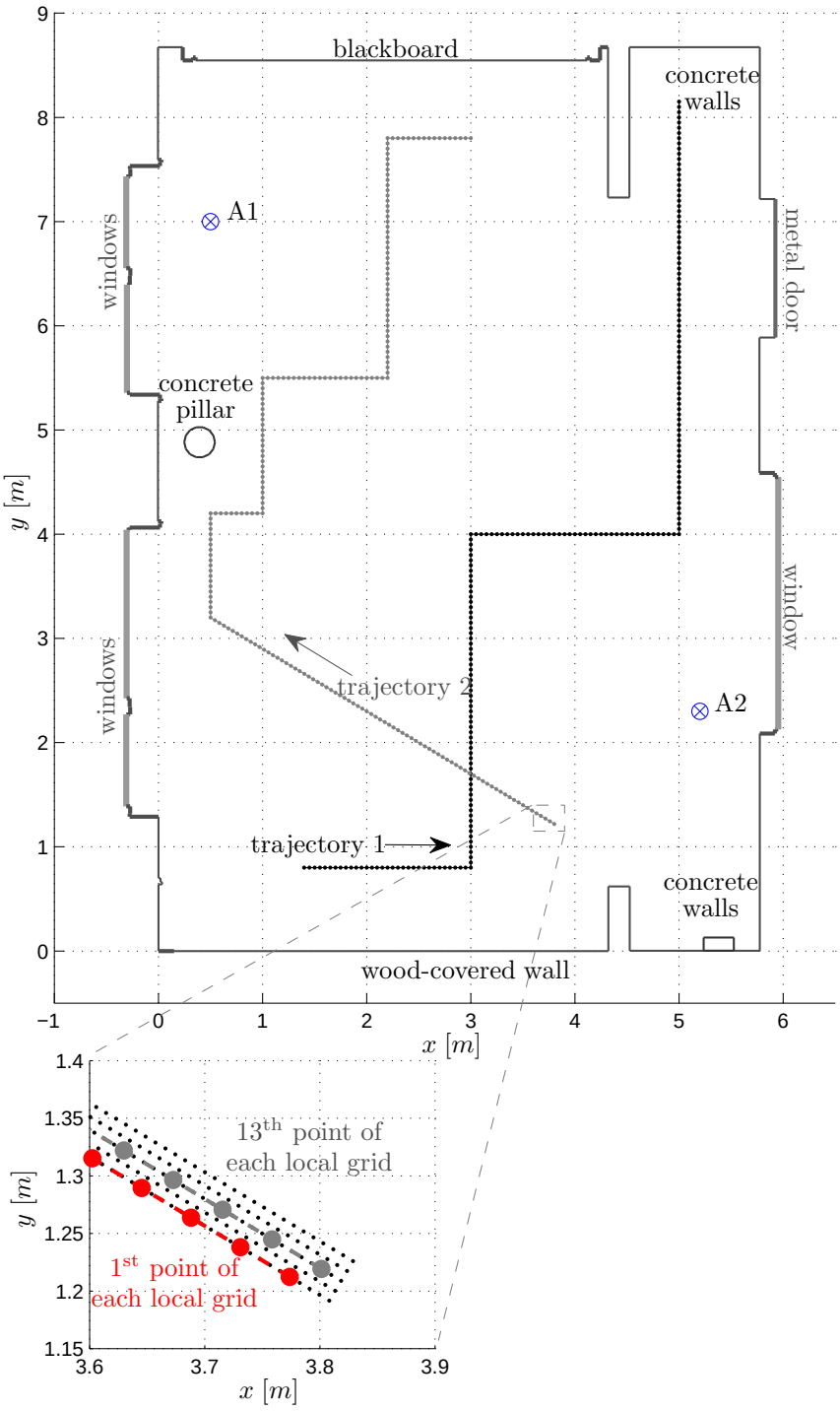

Figure 1.4: Medium-scale measurement scenario in a seminarroom of the laboratory. In this scenario, two anchors are available. Two different measurement setups are used: 1) Two trajectories with 220 points each, spaced by 5 cm, and 2) measurements within a local grids around each of the points of the two trajectories with 1 cm spacing. As the zoom plot on the bottom shows, this e.g. enables 25 parallel test trajectories or allows for spatial averaging for each trajectory point.

(a) Seminarroom, scenario

(b) Seminarroom, monostatic setup

Figure 1.5: Photo of Seminaroom scenario, view from the metal door at the lower side in Fig. 1.4.

Trajectory Measurements – VNA

The trajectory measurements have been performed with the VNA. 2x220 points with 5 cm spacing are available. Also, the 220 measurements between the two mobiles at each trajectory point are available. To obtain an additional set of measurements between the mobiles, the direction of mobile 2 has been reversed in the monostatic run.

Local Grid Measurements – M-sequence Radar

To enable a detailed local channel analysis for the two trajectories, grid measurements around them have been performed. Due to the large number of points, these have been obtained with the M-sequence radar, since it allows for much faster measurement times. Around each of the trajectory points, 5x5 points with a spacing of 1 cm have been used, hence in total, 11000 points are available. As can be seen in the lower plot of Fig. 1.4, this allows for e.g. 25 parallel test trajectories for tracking algorithms or to have multiple measurements around one point. The 13-th point of each local grid, i.e. the center point, corresponds to the respective measurement point in the trajectory measurements.

1.5.2 Demonstration Room at Graz University of Technology

Two measurement champaigns have been conducted in this room of our university (see Fig. 1.7 and Fig. **??**).

Scenario A

In this scenario two trajectories have been measured with the M-sequence radar. Trajectory 1 consists of 101 points, trajectory 2 of 235 points, each of them are spaced by 5 cm. The coin antennas were used for all anchors and mobiles.

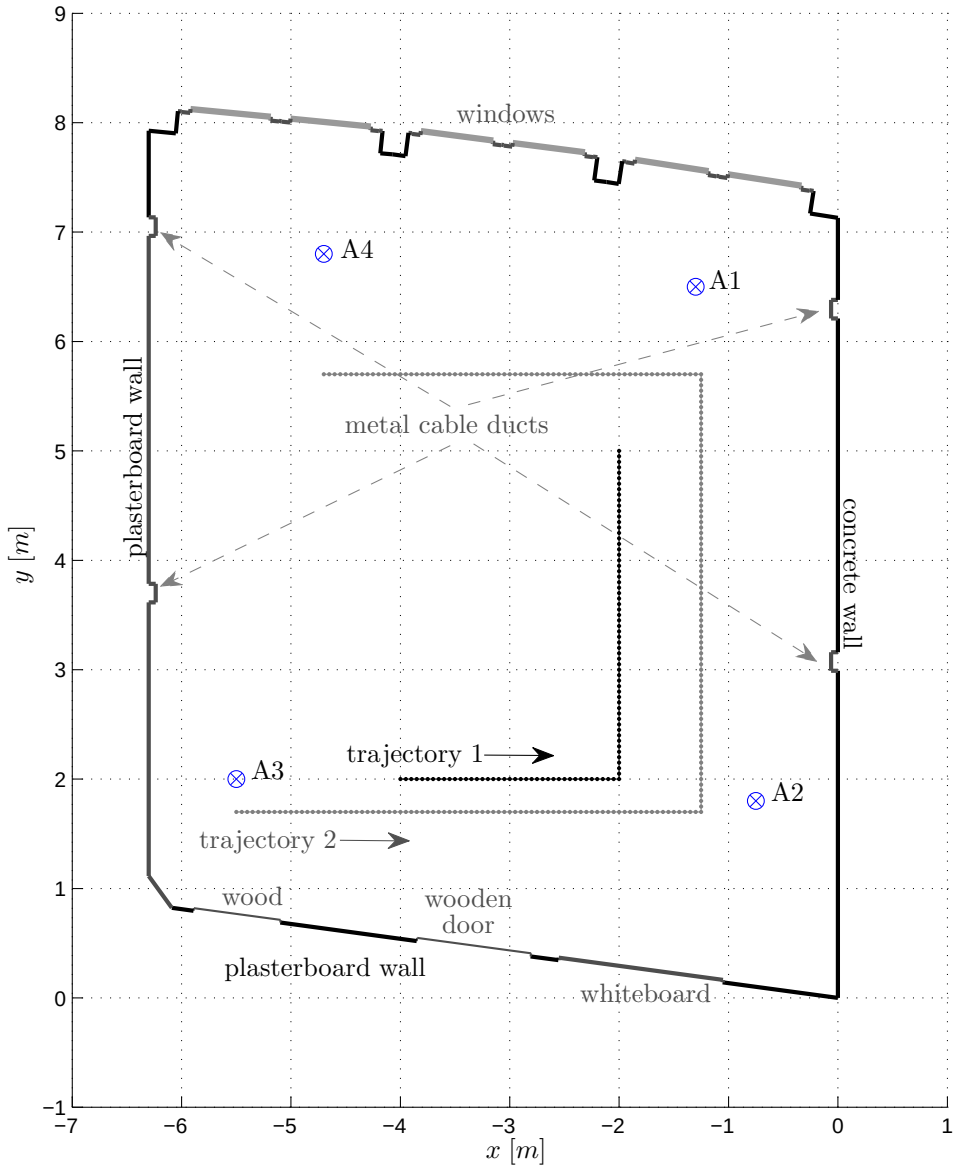

Figure 1.6: Medium-scale measurement scenario in a room (called the demonstration room) of the laboratory. In this scenario, four anchors are available and two trajectories with 101 and 235 points, respectively, spaced by 5 cm.

Scenario B

In this scenario four trajectories arranged on a rectangular grid with 1 cm spacing (66×71, i.e. in total 4686 measurement positions per trajectory) have been measured with the M-sequence radar and an automatic positioning table. The coin antennas were used for all anchors and mobiles.

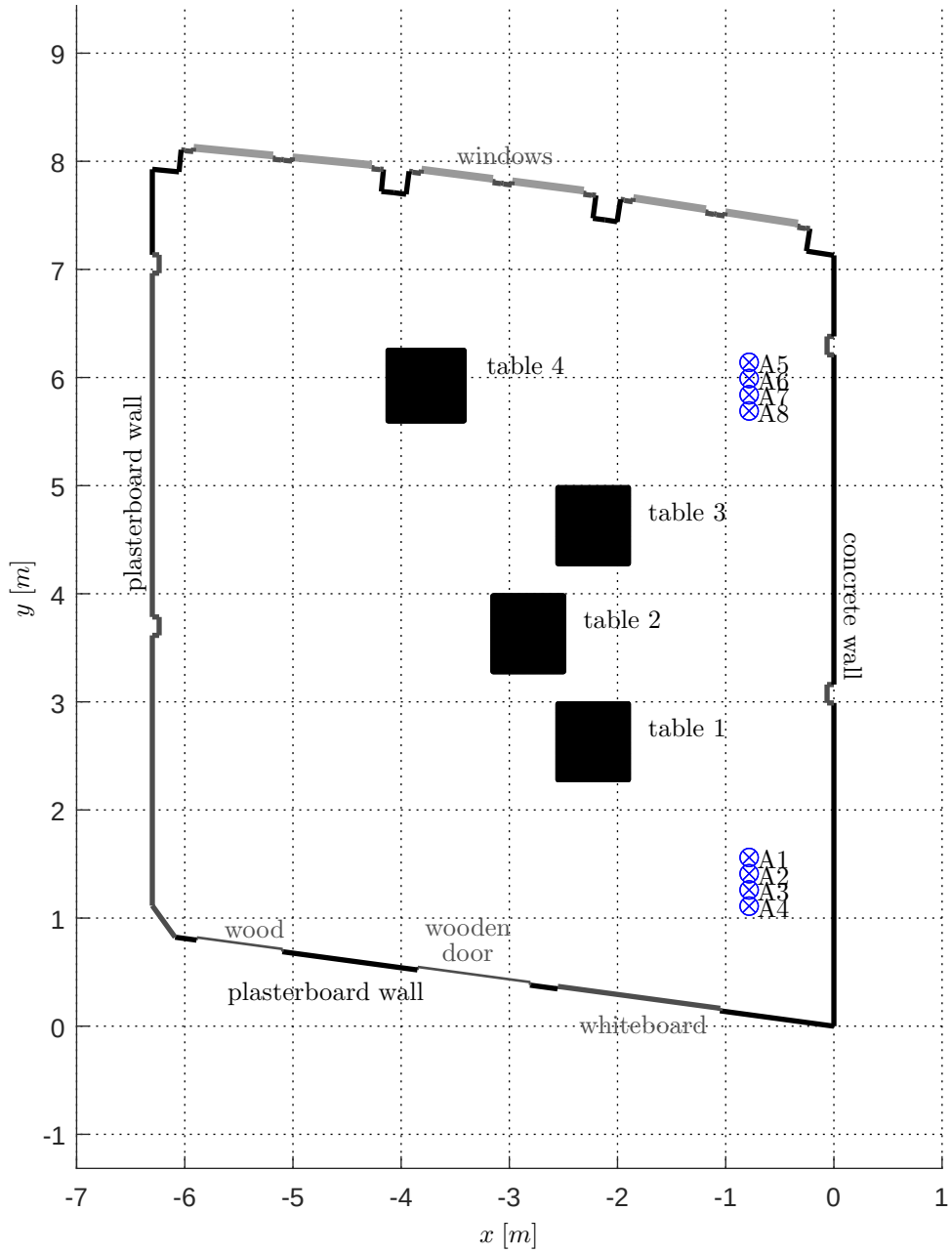

Figure 1.7: Medium-scale measurement scenario in a room (called the demonstration room) of the laboratory. In this scenario, eight anchors are available and four trajectories.

1.5.3 Demonstration Room at Montbeliard, France

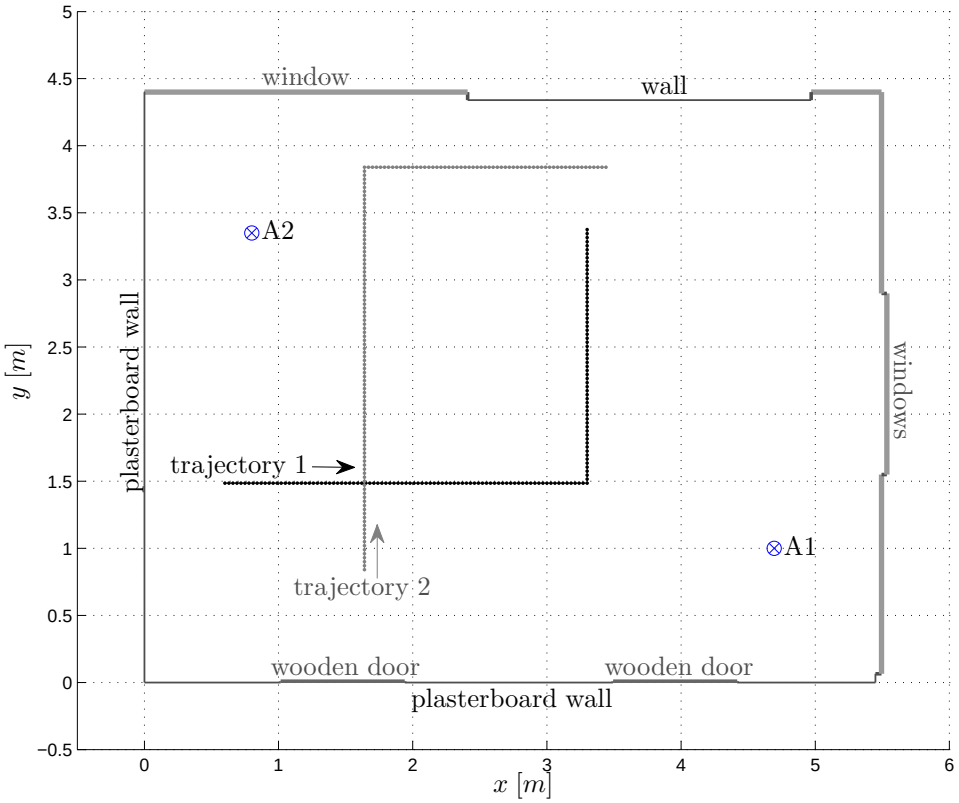

Figure 1.8: Medium-scale measurement scenario in a room (called the IPIN room) of the university in Monbeliard, France. In this scenario, two anchors are available and two trajectories with 154 and 161 points, respectively, spaced by 3 cm.

In this room of the university in Monbeliard, France, shown in Fig. 1.8, two trajectories have been measured with the M-sequence radar. Trajectory 1 consists of 154 points, trajectory 2 of 161 points, each of them are spaced by 3 cm. The coin antennas were used for all anchors and mobiles.

1.6 Small-Scale Environment – Laboratory Room

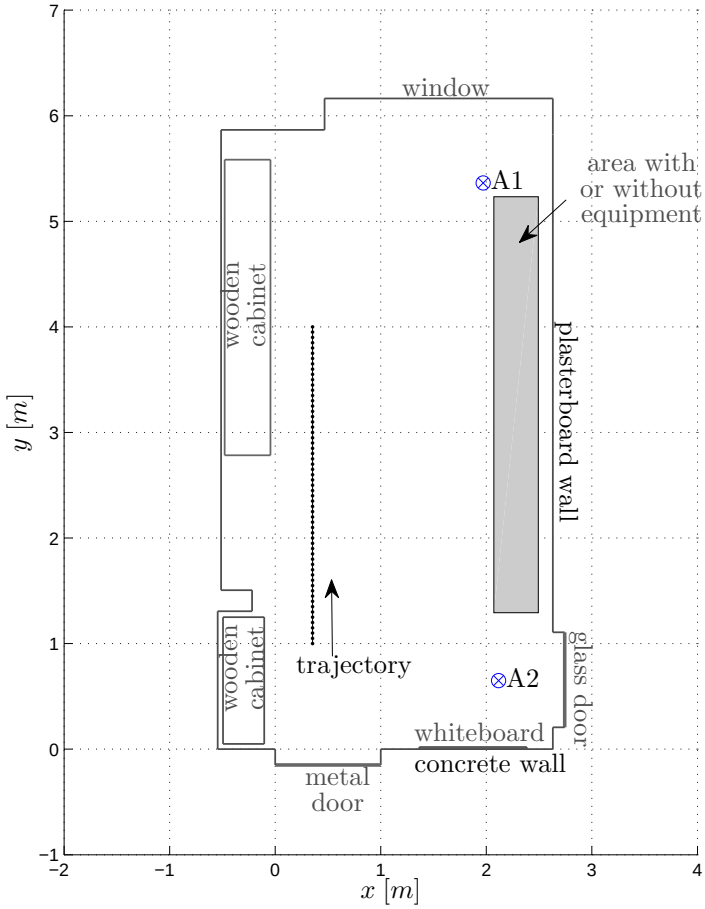

Figure 1.9: Small-scale measurement scenario in a laboratory room. In this scenario, two anchors are available and one trajectory with 60 points, spaced by 5 cm. In this scenario, the measurements have been done with the laboratory room rather empty, and once with all the measurement equipment in the room (mostly on tables within the gray area).

In this laboratory room of our university, shown in Fig. 1.9, test measurements were obtained with the VNA on a short trajectory of 60 points spaced by 5 cm. We have performed these measurements once with a rather empty room, and once with all the (mostly metallic) measurement equipment in it, see Fig. 1.10. This might be interesting for the evaluation of DM.

(a) Laboratory room, empty (b) Laboratory room, full

Figure 1.10: Photo of Laboratory room scenario, view from the metal door at the lower side in Fig. 1.9.

Bibliography

[CPB07] R. Cepeda, S. C J Parker, and M. Beach. The Measurement of Frequency Dependent Path Loss in Residential LOS Environments using Time Domain UWB Channel Sounding. In *Ultra-Wideband, 2007. ICUWB 2007. IEEE International Conference on*, 2007.

[FMGW11] M. Froehle, P. Meissner, T. Gigl, and K. Witrisal. Scatterer and Virtual Source Detection for Indoor UWB Channels. In *2011 IEEE International Conference on Ultra-Wideband (ICUWB 2011)*, Bologna, Italy, 2011.

[FMW12] M. Froehle, P. Meissner, and K. Witrisal. Tracking of UWB Multipath Components Using Probability Hypothesis Density Filters. In *2012 IEEE International Conference on Ultra-Wideband (ICUWB 2012)*, Syracuse, USA, 2012.

[Kra08] Christoph Krall. *Signal Processing for Ultra Wideband Transceivers*. Phd thesis, Graz Univ. of Techn. (Austria), 2008.

[Laf14] M. Lafer. Real-Time Multipath-Assisted Indoor Tracking and Feature Detection. Master's thesis, Graz University of Technology, 2014.

[LFMW14] E. Leitinger, M. Froehle, P Meissner, and K. Witrisal. Multipath-Assisted Maximum-Likelihood Indoor Positioning using UWB Signals. In *IEEE ICC Workshop on Advances in Network Localization and Navigation (ANLN)*, 2014.

[MAGW11a] P. Meissner, D. Arnitz, T. Gigl, and K. Witrisal. Analysis of an Indoor UWB Channel for Multipath-Aided Localization. In *IEEE International Conference on Ultra-Wideband (ICUWB)*, Bologna, Italy, 2011.

[MAGW11b] P. Meissner, D. Arnitz, T. Gigl, and K. Witrisal. Indoor UWB Channel Analysis in an Atrium-Style Office Building for Multipath-Aided Localization. In *COST Action IC1004 Scientific Meeting*, Lund, Sweden, 2011.

[MGM+13] P. Meissner, M. Gan, F. Mani, E. Leitinger, M. Froehle, C. Oestges, T. Zemen, and K. Witrisal. On the Use of Ray Tracing for Performance Prediction of UWB Indoor Localization Systems. In *IEEE ICC Workshop on Advances in Network Localization and Navigation (ANLN)*, Budapest, Hungary, 2013. invited paper.

[MLFW13] P. Meissner, E. Leitinger, M. Froehle, and K. Witrisal. Accurate and Robust Indoor Localization Systems Using Ultra-wideband Signals. In *European Navigation Conference (ENC)*, Vienna, Austria, 2013.

[MLLW13a] P. Meissner, M. Lafer, E. Leitinger, and K. Witrisal. Multipath-Assisted Indoor Navigation and Tracking. Live Demonstration at International Conference on Indoor Positioning and Indoor Navigation, IPIN, Montbéliard, France, 2013.

[MLLW13b] P. Meissner, E. Leitinger, M. Lafer, and K. Witrisal. MeasureMINT UWB database. www.spsc.tugraz.at/tools/UWBmeasurements, 2013. Publicly available database of UWB indoor channel measurements.

[MLLW14] P. Meissner, E. Leitinger, M. Lafer, and K. Witrisal. Real-Time Demonstration System for Multipath-Assisted Indoor Navigation and Tracking (MINT). In *IEEE ICC Workshop on Advances in Network Localization and Navigation (ANLN)*, Sydney, Australia, 2014.

[MLW14] P. Meissner, E. Leitinger, and K. Witrisal. UWB for Robust Indoor Tracking: Weighting of Multipath Components for Efficient Estimation. *IEEE Wireless Communications Letters*, 3(5):501–504, Oct. 2014.

[Mol05] A. Molisch. *Wireless Communications*. John Wiley & Sons, 2005.

[MW12a] P. Meissner and K. Witrisal. Analysis of Position-Related Information in Measured UWB Indoor Channels. In *6th European Conference on Antennas and Propagation (EuCAP)*, Prague, Czech Repuplic, 2012. convened session.

[MW12b] P. Meissner and K. Witrisal. Multipath-Assisted Single-Anchor Indoor Localization in an Office Environment. In *19th International Conference on Systems, Signals and Image Processing (IWSSIP)*, Vienna, Austria, 2012. invited paper.

[SHK+07] J. Sachs, R. Herrmann, M. Kmec, M. Helbig, and K. Schilling. Recent Advances and Applications of M-Sequence based Ultra-Wideband Sensors. In *IEEE International Conference on Ultra-Wideband, ICUWB 2007.*, 2007.

[SKA+10] T. Santos, J. Karedal, P. Almers, F. Tufvesson, and A. Molisch. Modeling the ultra-wideband outdoor channel: Measurements and parameter extraction method. *IEEE Transactions on Wireless Communications*, 9(1):282 –290, Jan. 2010.